Available online at www.sciencedirect.com
SCIENCE DIRECT®
Journal of Sound and Vibration 268 (2003) 581–599
JOURNAL OF SOUND AND VIBRATION
www.elsevier.com/locate/jsvi

An improved model of ER fluids in squeeze-flow through model updating of the estimated yield stress

A.K. El Wahed[a], J.L. Sproston[b], R. Stanway[c,*], E.W. Williams[d]

[a] *Department of Mechanical Engineering, University of Dundee, Dundee DD1 4HN, UK*
[b] *Department of Engineering, University of Liverpool, Liverpool L69, 3GH, UK*
[c] *Department of Mechanical Engineering, University of Sheffield, Mappin St., Sheffield S1 3JD, UK*
[d] *Department of Mathematical Sciences, University of Liverpool, Liverpool L69 7ZL, UK*

Received 15 February 2002; accepted 18 November 2002

Abstract

In the squeeze-flow mode of operation, electrorheological (ER) fluid is placed between two electrodes, which are free to translate in a direction roughly parallel to the direction of the applied electric field. Consequently, the ER fluid is subjected to alternate tensile and compressive strokes and shearing of the fluid also occurs. Available displacements are small but large forces are available from compact devices and there are many potential applications, notably in vibration isolation.

The present authors have spent several years developing mathematical models to account for the observed behaviour of ER fluids in squeeze-flow. Previous attempts at modelling squeeze-flow behaviour have been partially successful but there have always been discrepancies. These discrepancies have generally been attributed to the difficulty of estimating the yield stress developed within the ER fluid when an electric field is applied.

In the present paper, the authors describe a new approach in which the yield stress is determined iteratively by minimizing the difference between observed and predicted values of the transmitted force. Using this technique, force/displacement and force/velocity plots are predicted and compared with values from an experimental facility. It is shown that agreement between model predictions and experimental observation is excellent and significantly better than those obtained using existing models.

*Corresponding author. Tel.: +44-114-22-27728; fax: +44-114-22-27890.
E-mail addresses: a.elwahed@dundee.ac.uk (A.K. El Wahed), r.stanway@sheffield.ac.uk (R. Stanway).

0022-460X/03/$ - see front matter © 2003 Elsevier Ltd. All rights reserved.
doi:10.1016/S0022-460X(03)00374-2

1. Introduction

Electrorheological (ER) fluids are suspensions whose rheological properties can be substantially affected by an applied electric field. Specifically, when subjected to an electric field, flow only occurs after the imposition of a shear stress, which causes the ER fluid to yield. In general, the yield value (or yield stress) increases with increasing applied electric field.

Below the yield value, the ER fluid remains like a solid, although it may exhibit some creep. Above the yield value, flow will occur but it is plastic in nature. Accordingly, the well-known Bingham plastic model is often used at the starting point for explaining the rheological behaviour of ER fluids. Winslow [1] is credited with the first observation of the ER effect during his investigations into the application of high electrical fields across semi-conducting particulate suspensions. For a long time, ER fluids did not receive much scientific attention, mainly due to their slow response and inadequate yield stress in addition to their thermal and chemical instability. However, industrial applications of these fluids, during the last two decades, have seen considerable progress involving investigations into prototype and model devices. Vibration control is one of the most promising areas for the large-scale commercial exploitation of new ER fluids, which can provide damping forces to meet industrial requirements [2]. The first practical application of ER fluids in vibration control was reported in 1978 [3] in which a valve-operated vibration damper was described. Recently, the area of vibration control has seen a surge in the number of reported investigations particularly in engine mounts [4–6], primary shock absorbers [7–9] and rotor support systems [10] as well as in adaptive structures [11].

The majority of these investigations have employed the ER fluids in simple shear mode or flow mode of operation where the fluid is deformed in a direction normal to the arrays of particulate chains. An alternative arrangement, squeeze-flow, in which the fluid is subjected to compressive and tensile stresses in a direction parallel to the chains has been identified and investigated [12]. In this mode of operation, the fluid provides a yield stress that is an order of magnitude higher than that in the shear mode [13–15]. As a result, subsequent investigations, by the authors and other researchers, have focused on the performance of ER fluids in squeeze subjected to various mechanical and electrical inputs [16–23]. Comprehensive reviews of the literature, particularly in the classification of the modes of ER fluid operation and their potential engineering applications in vibration control have recently been reported [24–26].

Modelling of ER fluid behaviour is now relatively advanced especially for the flow mode [27] and shear mode [28] of operation. Progress has been made in developing models to account for squeeze-flow behaviour [15,16,21,29] but there still exist significant discrepancies between model predictions and experimental observations. It has been suggested that these discrepancies arise due to the difficulty of assigning a suitable value to the yield stress developed by an electrically exited ER fluid.

In what follows here, the authors describe a new approach to modelling ER fluids in squeeze-flow. The basic of the technique is the use of the now familiar bi-viscous model of the ER fluid. However, rather than use a power law or linear law model to estimate the yield stress, an iterative approach is used. Essentially the yield stress is updated so as to provide agreement between predicted and observed values of the force transmitted across the squeeze-flow cell. The approach draws on well-established techniques for the updating of dynamic models of engineering systems [30]. To provide the necessary platform for a discussion of the iterative technique, a summary of the existing theoretical model is given first.

2. Existing theoretical model

Fig. 1 shows a schematic view of an electrorheological fluid contained between two parallel circular electrodes of radius a. The lower electrode oscillates about its mean position ($z = 0$) with a displacement $y(t)$ whilst the upper electrode is fixed, for all time, at $z = y_0$. The theoretical modelling is directed towards the determination of the input force $F_1(t)$ and the transmitted force $F_2(t)$ from a set of experimental data for $y(t)$. These forces can then be compared with the values taken from the experimental facility.

The analysis presented here is based on a recent numerical investigation [29] in which the response of an automotive engine mount, having a similar electrode configuration to the one in the present investigation, was modelled successfully. This has been achieved by solving the quasi-steady equations for the fluid flow where the constitutive relationship is the bi-viscous model, which is described for a simple shear flow, Fig. 1, by

$$\tau(z) = \begin{cases} \eta_r \dfrac{\mathrm{d}u}{\mathrm{d}z} & \text{for } |\tau| < \tau_1, \\ \tau_0 + \eta \dfrac{\mathrm{d}u}{\mathrm{d}z} & \text{for } |\tau| > \tau_1. \end{cases} \tag{1}$$

The constants τ_0 and τ_1 are related by $\tau_0 = \tau_1(1 - \eta)$ where $\gamma = \eta/\eta_r$ (the ratio of the viscosities in the 'yielded' to the 'unyielded' regions) and u is the radial velocity of the fluid. Referring to the above analysis in which the fluid inertia and compressibility are neglected, the shear stress, τ, is then given by

$$\frac{\partial \tau}{\partial z} = \frac{\mathrm{d}p}{\mathrm{d}r}, \tag{2}$$

where $\mathrm{d}p/\mathrm{d}r$ is the radial pressure gradient. This equation is now solved subject to the no-slip conditions on the electrodes, given by $u(y_0) = u(y(t)) = 0$ together with the assumption that u and τ are continuous across the two yield surfaces in the fluid, which can be expressed as

$$z_1 = \frac{1}{2}\left(y_0 + y(t) + \frac{2\tau_1}{\mathrm{d}p/\mathrm{d}r}\right), \tag{3}$$

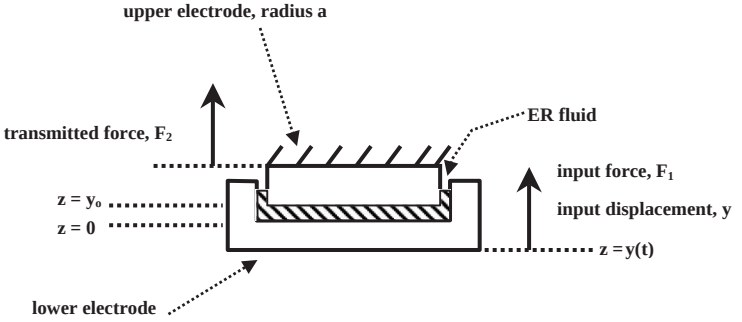

Fig. 1. ER squeeze flow cell.

$$z_2 = \frac{1}{2}\left(y_0 + y(t) - \frac{2\tau_1}{\mathrm{d}p/\mathrm{d}r}\right), \tag{4}$$

and the symmetry in the flow occurs about the mid-plane $z = (y_0 + y(t))/2$.

The radial velocity of the fluid is obtained by integrating Eq. (1) across the gap between the electrodes whilst the volumetric flow rate $2\pi rQ$ is obtained through the application of the continuity condition

$$2\pi rQ = 2\pi r \int_{z=y(t)}^{y_o} u \,\mathrm{d}z = \pi r^2 \dot{y}(t), \tag{5}$$

where $\dot{y}(t)$ is the vertical velocity of the lower electrode.

An equation for the pressure gradient $\mathrm{d}p/\mathrm{d}r$ is now available. In order to make this equation more accessible, the following two dimensionless variables

$$G = -\frac{(y_0 - y(t))}{2\tau_1}\left(\frac{\mathrm{d}p}{\mathrm{d}r}\right), \tag{6}$$

and

$$S = -\frac{\dot{y}(t)\eta r}{(y_0 - y(t))^2 \tau_1}, \tag{7}$$

are introduced for the radial pressure gradient and radius, respectively.

Williams et al. [29] reported that the physically acceptable solution of the radial pressure gradient G is given by a cubic equation in terms of S and γ

$$G^3 - 3\left[S + \tfrac{1}{2}(1-\gamma)\right]G^2 + \tfrac{1}{2}(1-\gamma) = 0. \tag{8}$$

The solution is only valid for the range of values of S where yield surfaces exist.

For non-zero values of γ and for sufficiently small radii, no yield surface occurs and the material in that neighbourhood behaves as a Newtonian fluid of viscosity η_r. For this case, the corresponding equation for the dimensionless pressure gradient is given by

$$G = \frac{3S}{\gamma}. \tag{9}$$

The primary objective here is to determine the average pressure p, over the upper electrode and therefore it is necessary to derive an expression for the transmitted force. This force is given by

$$F_2 = \int_{r=0}^{a} 2\pi r\, p(r)\,\mathrm{d}r = -\pi \int_{r=0}^{a} r^2 \frac{\mathrm{d}p}{\mathrm{d}r}\,\mathrm{d}r. \tag{10}$$

Integration over the upper electrode in addition to expressing Eq. (10) in terms of the non-dimensional variables, G and S, then give the transmitted force $F_2(t)$ in the form

$$F_2 = \frac{2\pi\tau_1 a^3 \phi(\chi)}{(y_0 - y(t))}, \tag{11}$$

where χ is the value of S at $r = a$

$$\chi = S(a) = -\frac{\dot{y}(t)\eta a}{(y_0 - y(t))^2 \tau_1}, \tag{12}$$

and the non-dimensional output force ϕ is

$$\phi = \frac{1}{108}\left(\frac{\gamma}{\chi}\right)^3 + \frac{1}{\chi^3}\int_{s=\gamma/3}^{\chi} S^2 G \, \mathrm{d}S. \tag{13}$$

When F_2 is obtained from Eq. (11) the input force F_1 is then calculated using Newton's second law applied to the lower electrode in the form

$$F_1 - F_2 = M\ddot{y}, \tag{14}$$

where M and $\ddot{y}$ are, respectively, the mass and acceleration of the lower electrode assembly.

3. Experimental arrangement

3.1. Experimental facility

The experimental facility, Fig. 2, consists of a Ling Dynamic Systems electromagnetic shaker (Model No. V450) which is capable of providing vertical oscillatory motion with a maximum amplitude of 19 mm (peak-to-peak) over a frequency range from zero to 7.5 kHz. The shaker head is attached rigidly to a Kistler (Model No. 9311A) piezoelectric force link and an earthed brass electrode having a recessed cylindrical cavity of diameter 95 mm which provides the reservoir for the ER fluid. The high voltage upper electrode is a circular brass disc of diameter 56 mm, its circumferential edge and rear face surrounded and supported by a PTFE collar. A second identical force link was rigidly connected between the PTFE collar and the supporting frame. However, the initial inter-electrode gap could be changed via a positioning assembly without compromising the rigidity of the top assembly.

The instantaneous displacement of the lower electrode is determined using an RDP (type GTX 2500) LVDT, the velocity using an RDP (Type 240A0500) self-induced velocity sensor and the acceleration using an Endevco (Type 7254-100) accelerometer, all three devices attached to the

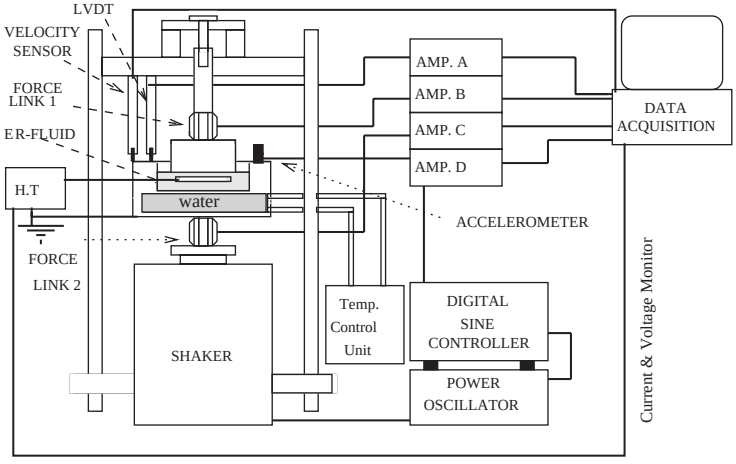

Fig. 2. Experimental arrangement.

upper surface of the lower electrode. Electrical excitation of the ER fluid is achieved by means of a Trek (Model 664) high voltage amplifier, driven by a Thander (Model TG102) function generator. High voltage sinusoidal, square and triangular waveforms with 40 kHz bandwidth are available in addition to the optically isolated current monitoring facility. Data acquisition and processing are achieved using a Measurement Group (Type ESAM) analogue-to-digital converter that is controlled by a Pascal program running on an IBM-compatible personal computer. Feedback control was not imposed in these tests but could be achieved, if required, using a Ling Dynamic Systems (Model DSC4) digital sine controller employing as input the signal from the accelerometer. In order that meaningful comparisons could be made between the results of the various tests, the ER fluid temperature was controlled by re-circulating water through a second closed cavity in the lower electrode using a Grant Instruments (Model LTD6) temperature controller.

3.2. Calibration of sensors

The two force links were calibrated statically by sequential loading using small weights, while the LVDT was calibrated using a dial gauge. The accelerometer, pre-calibrated by the manufacturer, was found to function as specified to within $\pm 0.6\%$ when its maximum transverse sensitivity was checked using the digital sine controller. As an additional check, the displacement signal from the LVDT was differentiated twice using central differences and the resulting signal was found to compare well with that from the accelerometer. Finally the data acquisition system was checked against a DC signal supplied by a millivolt calibration unit (Time Electronics Ltd., Model 404S) and was found to be accurate to within $\pm 0.5\%$.

3.3. ER fluid composition

The ER fluid used in this investigation is a suspension of agglomerated corn flour in silicone oil. The solid phase was supplied with an average diameter of 90 μm and was subsequently ground and sieved, using an Endecots Ltd. laboratory test sieve system in conjunction with a Fritsch analysette (type 03502) mechanical vibrator, to produce particles in the range from 10 to 28 μm. The kinematic viscosity of the oil at 20°C was 10 cSt and the weight fraction of the solid phase was chosen as 57%. The electrical conductivity of the solid phase was measured in a dedicated cell and found to be 3.36×10^{-10} S/m.

4. Experimental results and comparison with existing theory

The tests carried out consisted of the simultaneous measurement of the instantaneous values of the input force delivered by the shaker, the transmitted force across the ER fluid, the displacement, velocity and acceleration of the lower electrode together with the current through the fluid and the applied voltage. These measurements were collected at a sampling frequency of 5 kHz for a range of mechanical frequencies, for DC excitation and for several values of the applied voltage. The input displacement amplitude of the lower electrode, for the electrically unstressed fluid, was chosen as 0.4 mm for each mechanical frequency (i.e., 20% of the initial

inter-electrode gap of 2 mm). However, the amplitude reduces with applied voltage and is therefore not controlled in the present tests. The fluid temperature was maintained at 30°C throughout and this was found necessary in order to compare results of different tests.

For a mechanical frequency of 8 Hz, the variation in input displacement and velocity of the lower assembly together with the input force delivered by the shaker and the transmitted force across the ER fluid for zero voltage is presented in Fig. 3. It can be seen that the maximum value of the transmitted force occurs when the lower assembly passes through its mean position and travels with its maximum velocity. The effect of applying a potential difference of 4 kV can be seen clearly in Fig. 4 where the maximum input displacement is reduced by a factor of 15, in comparison with the zero-voltage case, to 27 μm. This is accompanied by a maximum velocity

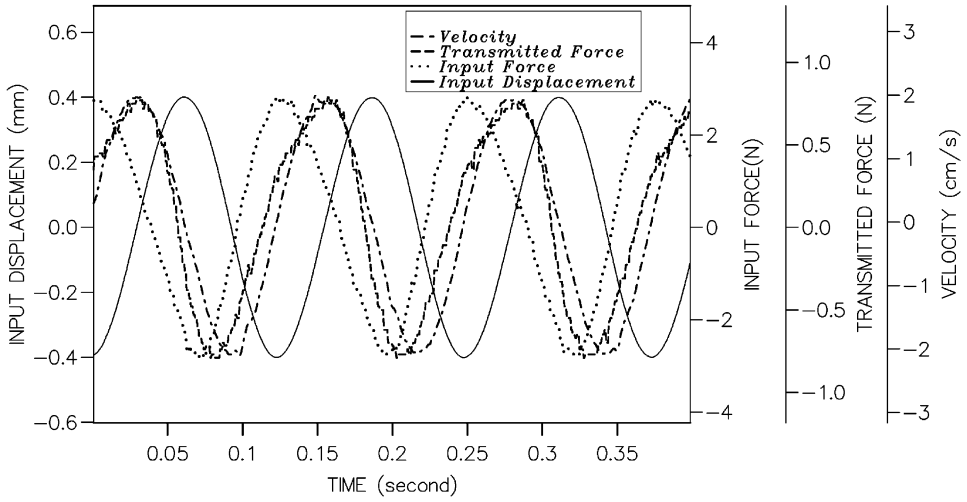

Fig. 3. ER Fluid in squeeze under constant voltage (mechanical frequency = 8.0 Hz; applied voltage = 0.0 kV).

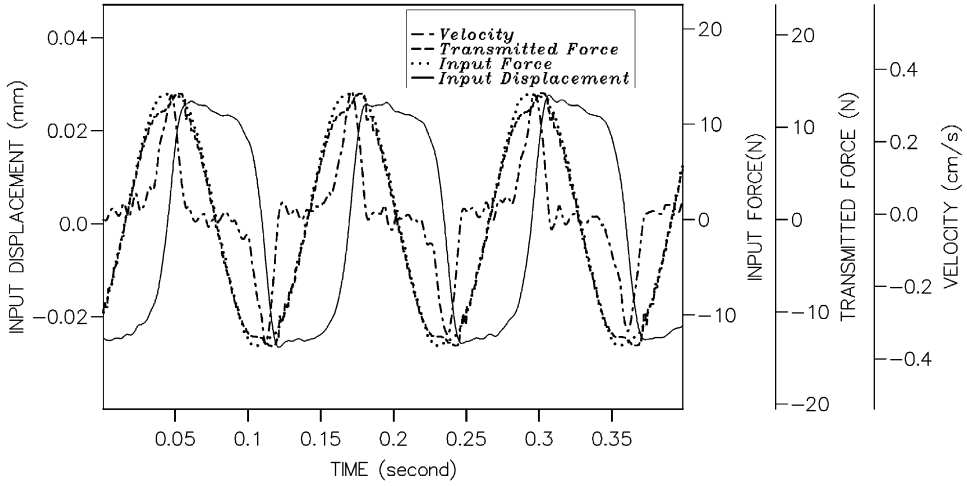

Fig. 4. ER Fluid in squeeze under constant voltage (mechanical frequency = 8.0 Hz; applied voltage = 4.0 kV).

reduction by a factor of about 6. Fig. 4 also shows that the lower assembly is brought to a halt for about 50 ms when it reaches its highest or lowest possible position, which is represented by an almost flat line imposed on the input displacement and velocity signals.

It is noted that the higher the applied voltage the longer is the rest period. This is considered to be an important factor that needs to be taken into account when a vibration control device, employing ER fluid in squeeze, is designed. It is also shown that the transmitted force coincides, in amplitude and phase, with the input force, Fig. 4, confirming the development of a high yield stress when the fluid is energized by sufficiently high voltage in contrast to the 18 ms lag time that appears to lapse before the input force is transmitted across the fluid (zero-voltage case), Fig. 3.

The variation of the input displacement and the force transmissibility, defined as the ratio of transmitted to input force, as a function of applied voltage are shown, respectively, in Figs. 5 and 6 for two mechanical frequencies, namely 8 and 15 Hz. It can be seen in Fig. 5 that the input displacement varies almost linearly with the applied voltage when it is in excess of 1 kV. When the maximum voltage is applied, the force transmissibility has a value very close to unity, Fig. 6, implying that the fluid develops a solid-body characteristic by which the motion of the shaker is almost arrested. However, the force transmissibility is less for the case of 15 Hz, which is due to the fact that the shaker provides a higher force level when it is operated at a higher mechanical frequency for the same input displacement [20] and as a result, 4.5 kV was required to stop the shaker. This happened despite using a bigger shaker capable of supplying a peak force of 500 N in comparison with 200 N provided by the shaker, which was used by the authors in their previous investigations. However, Table 1 shows a comparison between the above variables for the two cases when the fluid was excited by 0.0 and 4.0 kV.

The behaviour of the ER fluid cell was compared with that predicted by the bi-viscous model, and the results are shown in Fig. 7 for one force cycle for the case of 1 kV. In this figure, the experimental and theoretical data for the transmitted force seem to compare well when the lower assembly approaches its stationary position but the agreement becomes poor when the lower assembly travels

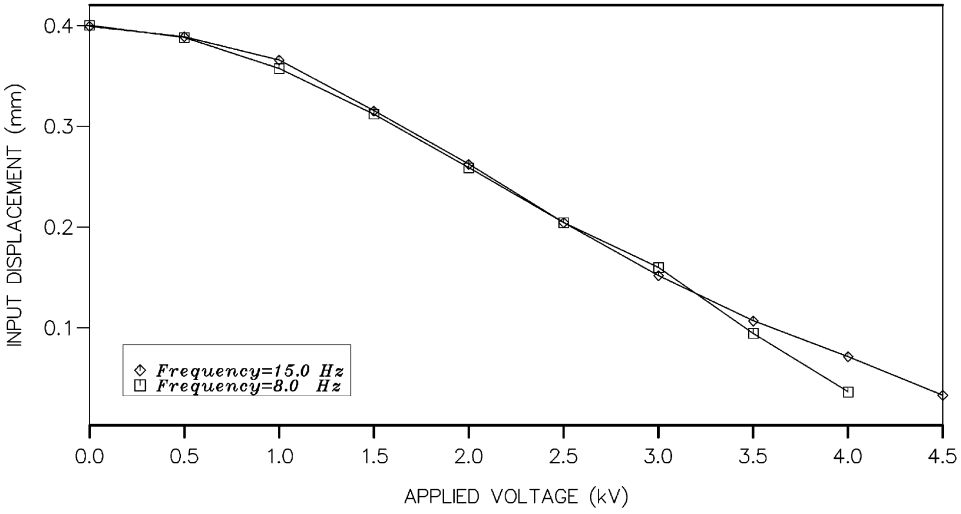

Fig. 5. Input displacement versus applied voltage.

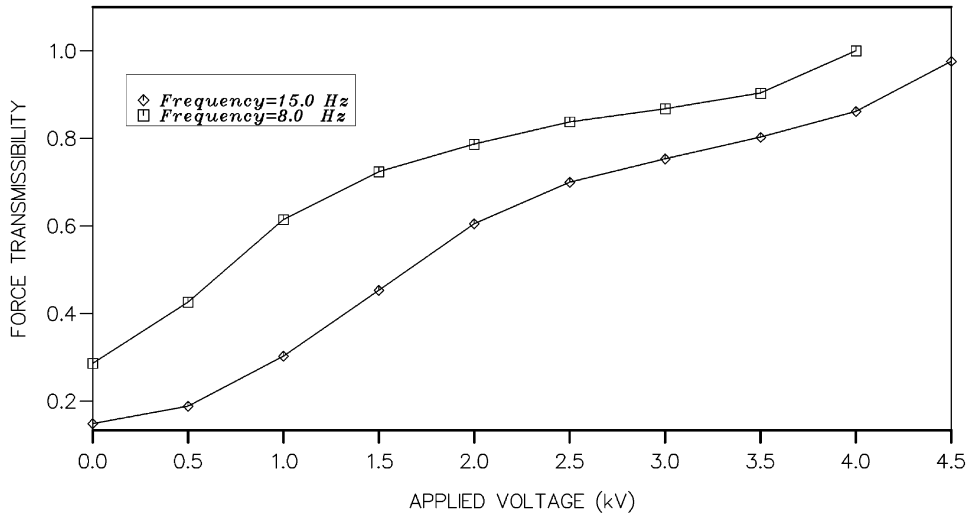

Fig. 6. Force transmissibility versus applied voltage.

Table 1
ER fluid performance under zero and 4.0 kV applied voltage

		8 Hz	15 Hz
0.0 kV	Input displacement (mm)	0.4	0.4
	Input force (N)	2.79	10.39
	Transmitted force (N)	0.78	1.56
4.0 kV	Input displacement (mm)	0.0267	0.0675
	Input force (N)	13.18	14.8
	Transmitted force (N)	13.12	12.84

with its maximum velocity. This was also the case when the performance of a similar ER cell, driven by a smaller shaker, was simulated using the current theory [17,19]. Consequently, it was decided to investigate ways of improving the model so that predictions would compare well with observed values. Attention was focused upon the estimation of the yield stress, τ_1.

5. Towards an improved mathematical model

5.1. Estimation of yield stress using power law and linear law models

In the previous investigations, the yield stress, τ_1, has been estimated using a power law model of the form

$$\tau_1 = AE^b, \tag{15}$$

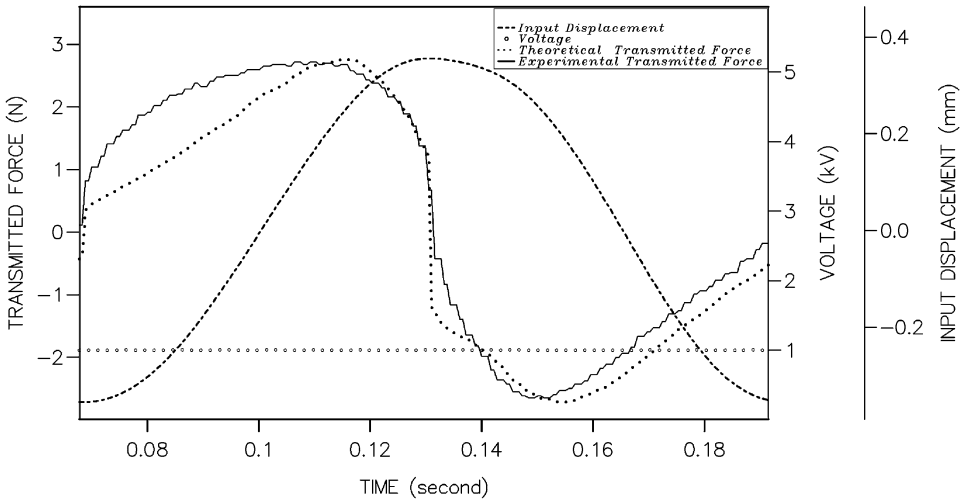

Fig. 7. Variation of transmitted force with time (mechanical frequency = 8.0 Hz).

where the constants A and b are system dependent, and E is the electric field strength. In the present investigation the value of b was taken to be 2.2, which is within the useful range 2–2.4 [31]. This law was specifically derived for an ER fluid in shear when the gap between the shearing electrodes is fixed; the situation here is more complex as the fluid is subjected to compressive and tensile loading in which the gap and hence the electric field continuously change. Moreover, the existence of more than one kind of yield stress of ER fluids whose value depends on whether the fluid is in a state of static or dynamic stress has been demonstrated [32].

Recent investigations carried out by the authors [16,21,29] have demonstrated the accuracy of the present theory for the case of a Newtonian fluid ($\gamma = 1$), where the fluid yield stress τ_1, becomes redundant. As a result it was thought prudent to consider modifying the way in which the yield stress of the ER fluid in squeeze is determined, in order to achieve better agreement with the experimental results. A recent investigation [33] has highlighted the advantages of a new technique in which the yield stress is determined using two different formulae, namely the power-law (Eq. (15)) and a linear-law, each of which is applicable over a specific limited range of applied fields. The piece-meal representation of the yield stress adopted by Bose et al. [33] is applied in the present investigation and the linear equation takes the form

$$\tau_1 = \tau_{e0} + \frac{\tau_{e0}}{E_0} E, \tag{16}$$

where τ_{e0} is an offset, which represents the lowest value of the yield stress calculated over an electric field range, the start of which is marked by E_0, using Eq. (16).

The results are shown in Fig. 8 in which the agreement between the predicted and the experimental results show little or no improvement over the results in Fig. 7.

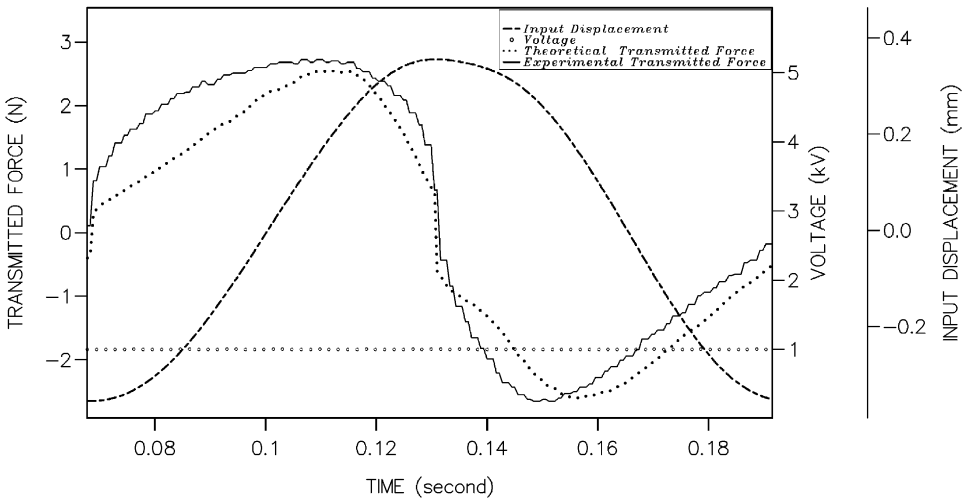

Fig. 8. Variation of transmitted force with time (mechanical frequency = 8.0 Hz).

5.2. Model updating of the estimated yield stress

As a result, it was decided to estimate the yield stress using a combination of the present algorithm as well as the experimental values of input displacement and transmitted force. The iterative procedure is illustrated in the flow chart, Fig. 9. First, the computer program based on the present theory is used to estimate the instantaneous values of the yield stress using the power-law, Eq. (15)

$$\tau_1 = AE^b,$$

which are then used to determine the transmitted force, Eq. (11)

$$F_2 = \frac{2\pi\tau_1 a^3 \phi(\chi)}{(y_0 - y(t))}.$$

Second, successive iterations are then performed in order to achieve sufficiently close agreement between the predicted and experimental values of the transmitted force. During each of these iterations, a new χ value is calculated using Eq. (12)

$$\chi = S(a) = -\frac{\dot{y}(t)\eta a}{(y_0 - y(t))^2 \tau_1}.$$

This new χ value is based on the updated yield stress determined using Eq. (11), in which the experimental results are substituted for F_2.

The instantaneous yield stress values that satisfied the above condition are shown in Figs. 10 and 11 as a function of time and applied field, respectively. The yield stress determined using the power-law is also shown. It can be seen that the yield stress reaches its minimum value when the lower assembly (electrode) approaches its stationary position and this confirms the fact that the yield stress provides the resistance to flow or deformation. However, the yield stress results, which are based on the power-law, reach their maximum value about the above electrode position and this would explain the relatively poor agreement between the predicted and the experimental

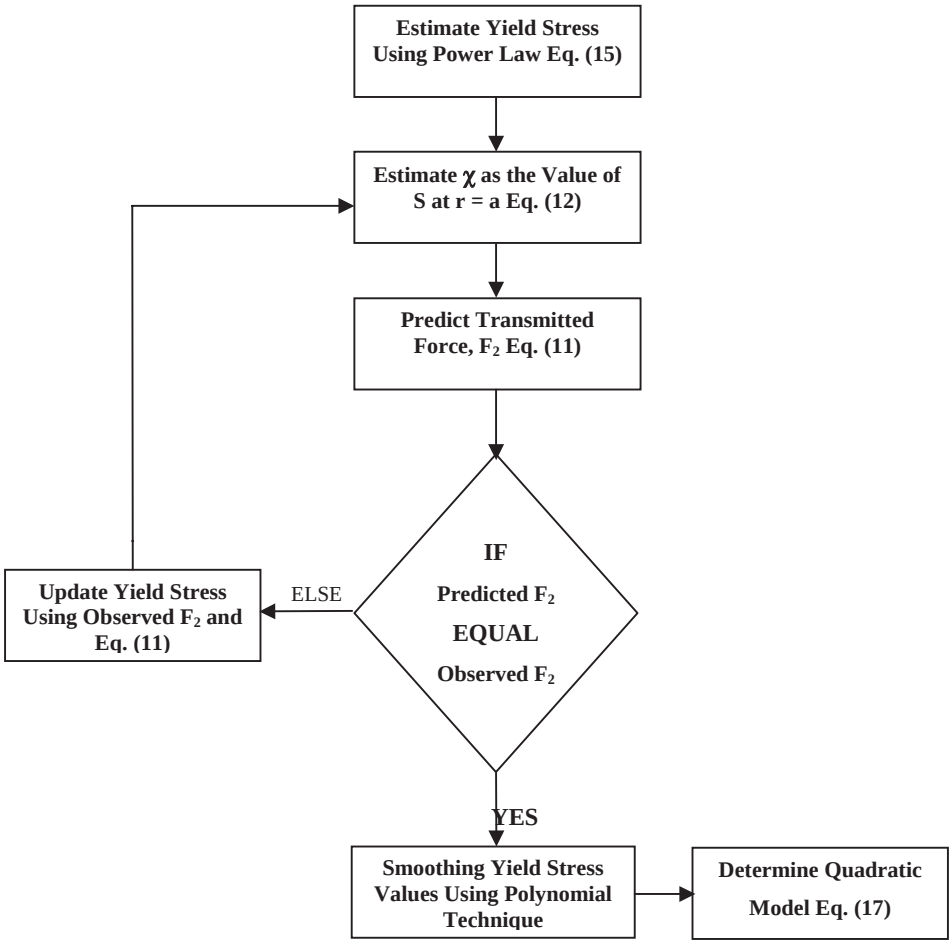

Fig. 9. Block diagram showing the iterative technique.

results. In these figures, it is also seen that the new yield stress, developed by the fluid, is higher when the ER fluid is in tension. This might be attributed to the fact that the electrostatic attraction forces between the particles is sufficient to prevent them from being pulled apart (tensile phase) whilst they would slide on each other during the compression phase.

5.3. A quadratic model for estimating yield stress

A program that incorporates smoothing through polynomial fitting [34] was used to determine the best equation to simulate the new yield stress data. This is shown on the flow chart, Fig. 9. From this, a quadratic equation was found which was of the form

$$\tau_1 = c + \frac{d}{E} + \frac{e}{E^2}, \tag{17}$$

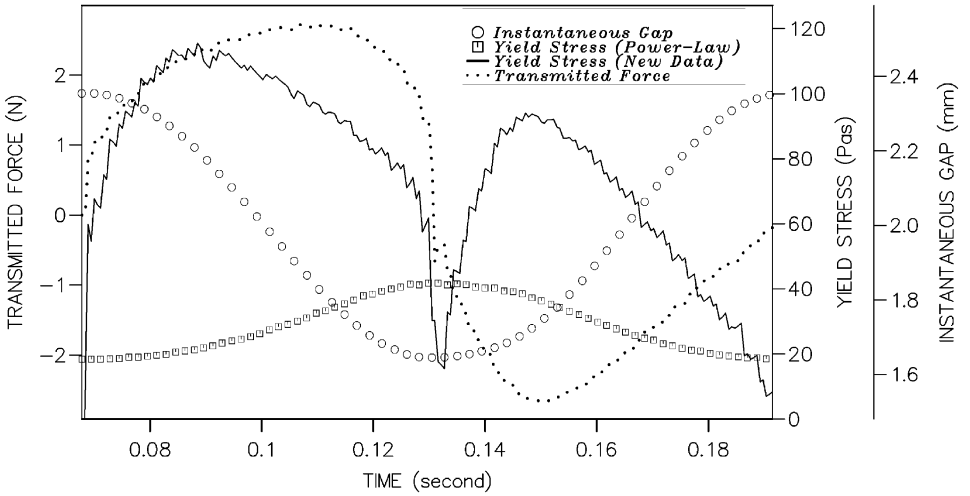

Fig. 10. Rheological behaviour of ER Fluid cell (mechanical frequency = 8.0 Hz; applied voltage = 1.0 kV).

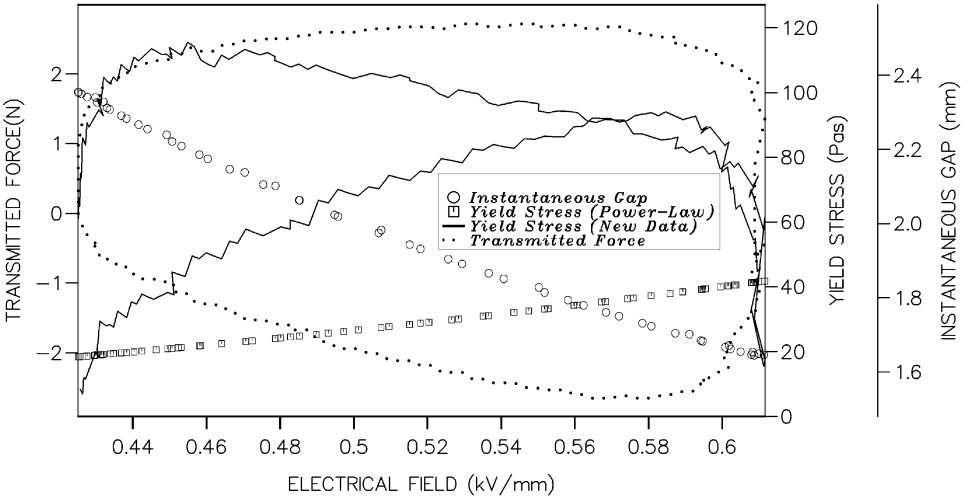

Fig. 11. Rheological behaviour of ER Fluid cell (mechanical frequency = 8.0 Hz; applied voltage = 1.0 kV).

where c, d and e are constants whose magnitude and sign are dependent on the direction of strain (compression or tension). The response of the ER cell energized by 1 kV was then assessed using the present theory in conjunction with the newly derived yield stress formula and the results are shown in Fig. 12 for the transmitted force F_2.

The predicted values of the input force F_1, shown in Fig. 13, in general closely resemble the experimental data apart from the noise imposed on the former due to the noisy acceleration data used to determine their instantaneous values (Eq. (14)).

The variation of the transmitted force with instantaneous inter-electrode gap and velocity for an electrical excitation of 1 kV is shown in Figs. 14 and 15, respectively, for the cases when the yield stress is determined using the power-law, linear/power-law and quadratic equations.

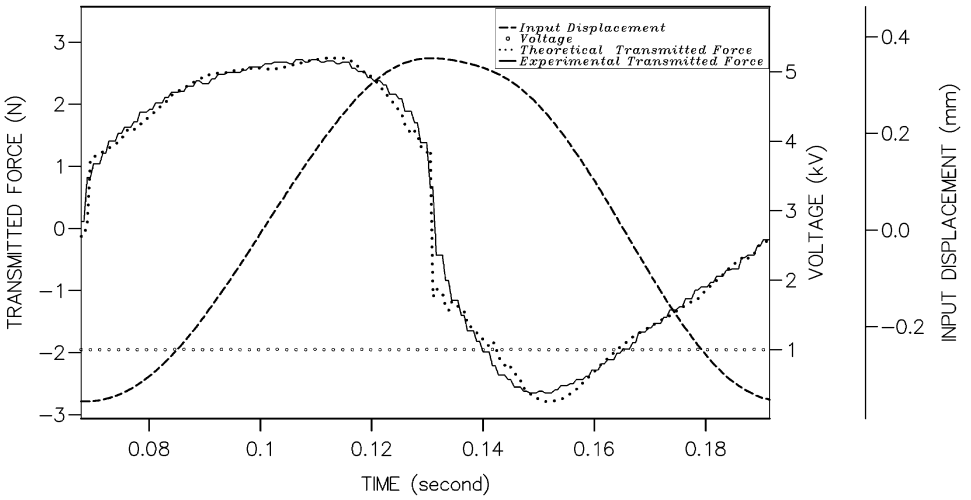

Fig. 12. Variation of transmitted force with time (mechanical frequency = 8.0 Hz)

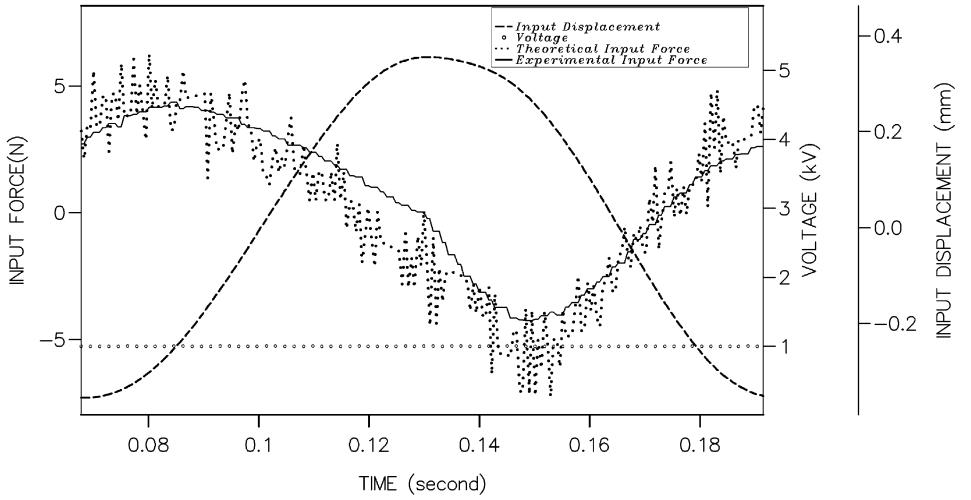

Fig. 13. Variation of input force with time (mechanical frequency = 8.0 Hz).

It can be seen that the data predicted using the quadratic formula, Eq. (17), compare extremely well with the experimental results whilst the power law, Eq. (15), and the linear/power law, Eqs. (16) and (15), produce predictions which agree with the experimental results only when the lower assembly approaches its stationary position. This suggests that the power-law equation might become applicable when the fluid is subjected to near-static loading and thus the gap can be assumed to be constant for a short period of time.

It is worth mentioning that the present theory featuring the new quadratic yield stress equation has been used to predict the performance of the ER cell for a range of applied voltages [35] and the results are in excellent agreement with the experimental data.

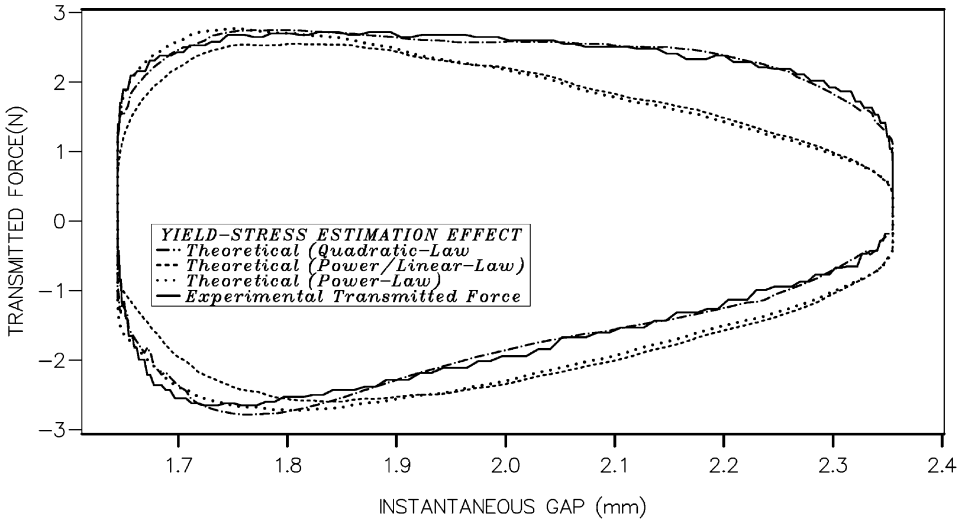

Fig. 14. Transmitted force versus instantaneous gap (mechanical frequency = 8.0 Hz; applied voltage = 1.0 kV).

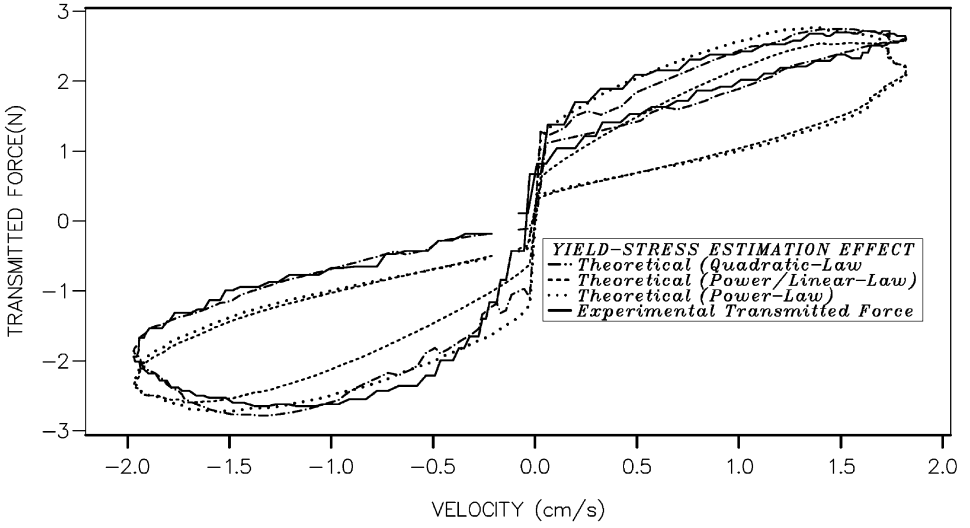

Fig. 15. Variation of transmitted force with velocity (mechanical frequency = 8.0 Hz; applied voltage = 1.0 kV).

The estimated yield stress using the quadratic formula for applied voltages in the range 0.5–3.5 kV is shown in Fig. 16 as a function of instantaneous gap and in Fig. 17 as a function of velocity. In both figures, the unsymmetrical nature of the yield stress with the strain direction is clearly shown. This data should prove useful for design purposes when the control of an ER fluid squeeze-flow device is considered.

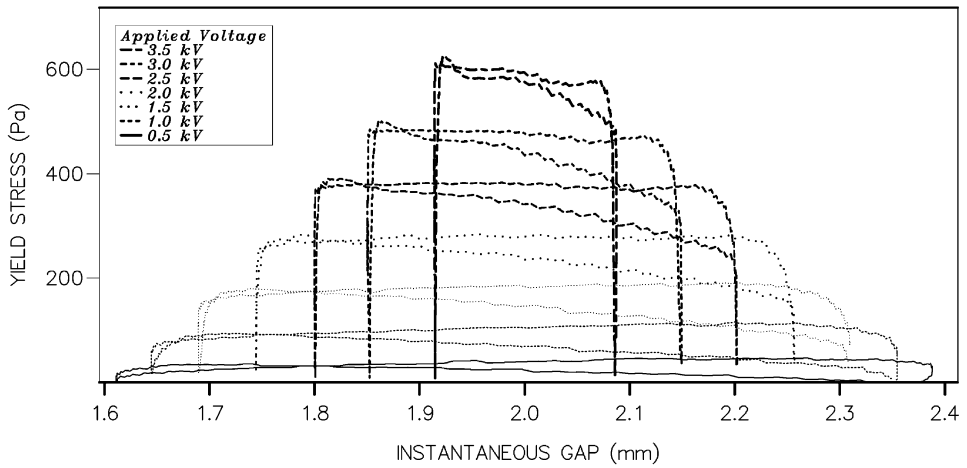

Fig. 16. Yield stress versus instantaneous gap (mechanical frequency = 8.0 Hz).

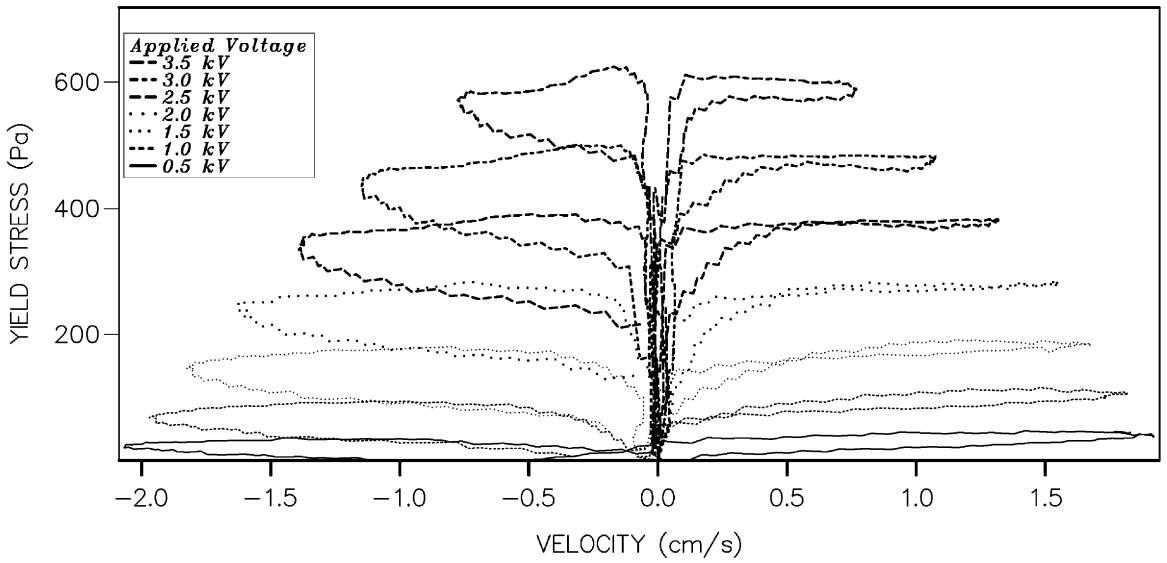

Fig. 17. Variation of yield stress with velocity (mechanical frequency = 8.0 Hz).

6. Conclusions

In this paper, the authors have described an extension to an existing technique for modelling the behaviour of an ER squeeze-flow cell under dynamic conditions. The key to the new approach lies in the iterative calculation of the yield stress, which is developed within the fluid when an electric field is applied. The iterative technique works to force agreement between the transmitted force predicted by the model and that measured experimentally. It is shown that this approach results in

a quadratic model relating yield stress to applied electric field. Experiments have been described which demonstrate that the quadratic model provides significantly better agreement between model predictions and observations.

The optimized theoretical model reported here would be used to predict the performance of ER fluid in squeeze. The obvious application of such fluids is in vibration control devices, which are employed by the automotive and aerospace industries.

Acknowledgements

This work is supported by EPSRC research grant GR/M25407.

Appendix A. Nomenclature

A constant in Eq. (15)
a radius of electrodes
b constant in Eq. (15)
c, d, e constants in Eq. (17)
E electric field strength
E_0 constant in Eq. (16)
F_1 input force
F_2 output (or transmitted) force
G dimensionless radial pressure gradient defined in Eq. (6)
M mass of lower (oscillating) assembly
p local pressure
Q volumetric flow rate/$2\pi r$
r radial co-ordinate
S dimensionless radial variable defined in Eq. (7)
t time
u radial velocity of fluid
z instantaneous inter-electrode gap ($z = y(t)$)
z_1, z_2 two yield surfaces in the fluid
χ dimensionless disk radius defined as the value of S at $r = a$, Eq. (12)
y displacement of lower electrode
y_0 initial (mean) separation of electrodes
$\dot{y}$ velocity of lower electrode
$\ddot{y}$ acceleration of lower electrode
γ $= \eta/\eta_r$
η, η_r post and pre-yield fluid viscosities
τ shear stress
τ_0, τ_1 fluid yield stress
τ_{e0} constant in Eq. (16)
ϕ non-dimensional output force

References

[1] W.M. Winslow, Induced fibration of suspensions, Journal of Applied Physics 20 (1949) 1137–1140.
[2] D.L. Hartsock, R.F. Novak, G.J. Chaundy, Electrorheological fluid requirements for automotive devices, Journal of Rheology 35 (1991) 1305–1326.
[3] W.A. Bullough, M.B. Foxon, A proportionate Coulomb and viscously damped isolation system, Journal of Sound and Vibration 56 (1978) 35–44.
[4] N.K. Petek, R.J. Goudie, F.P. Boyle, Actively controlled damping in electrorheological fluid-filled engine mounts, SAE Technical Paper No. 881785, 1988.
[5] J.H. Spurk, R. Muenzing, Anti-vibration mount with ER-fluid, American Society of Mechanical Engineering, Fluids Engineering Division (Publication) FED 205 (1994) 51–56.
[6] S. Morishita, T. Tsuchiya, T. Yoshioka, H. Johjima, T. Wade, Y. Ogasawara, Characteristics of controllable vibration-proof mount using liquid crystal, Transactions of the Japan Society of Mechanical Engineers, C 63 (1997) 3778–3783.
[7] W.A. Bullough, D.J. Peel, J.L. Sproston, R. Stanway, An ER long-stroke damper for vehicle suspension applications, American Society of Mechanical Engineers, Fluids Engineering Division Publication FED (Developments in ER Flows and Measurement Uncertainty) 205 (1994) 41–49.
[8] M. Nakano, T. Yonekawa, Active damper using electrorheological suspension and its application to vibration control, Noise and Vibration Worldwide 28 (8) (1997) 21–29.
[9] N.M. Wereley, J. Lindler, Biviscous damping behaviour in electrorheological dampers, in: G. Washington, J. Redmond (Eds.), 1999 Adaptive Structures and Material Systems, Vol. 59, Nashville, TN, 1999, ASME, New York, pp. 67–75.
[10] G.Z. Yao, Y. Qiu, G. Meng, T. Fang, Y.B. Fan, Vibration control of a rotor system by disk type electrorheological damper, Journal of Sound and Vibration 219 (1999) 175–188.
[11] R. Ehrgott, S.F. Masri, Modeling the oscillatory dynamic behaviour of electrorheological fluids in shear, Smart Materials and Structures 1 (4) (1992) 275–285.
[12] R. Stanway, J.L. Sproston, M.J. Prendergast, J.R. Case, C.E. Wilne, ER fluids in the squeeze-flow mode: an application to vibration isolation, Journal of Electrostatics 28 (1992) 89–94.
[13] G.J. Monkman, The electrorheological effect under compressive stress, Journal of Physics D 28 (1995) 588–593.
[14] H. Gong, M.K. Lim, Experimental investigations on tension and compression properties of an electro-rheological material, Journal of Intelligent Material Systems and Structures 7 (1996) 89–96.
[15] A. Lukharinen, K. Kaski, Computational studies of compressed and sheared electrorheological fluid, Journal of Physics D 29 (1996) 2729–2732.
[16] J.L. Sproston, R. Stanway, E.W. Williams, S.G. Rigby, The electrorheological automotive engine mount, Journal of Electrostatics 32 (1994) 253–259.
[17] J.L. Sproston, A.K. El Wahed, E.W. Williams, R. Stanway, A comparison of the performance of ER fluid in squeeze, International Journal of Modern Physics B 10 (23 & 24) (1996) 3081–3091.
[18] J.L. Sproston, A.K. El Wahed, R. Stanway, Electrorheological fluids in squeeze under AC and DC excitation, International Journal of Modern Physics B 13 (14, 15 & 16) (1999) 1861–1869.
[19] A.K. El Wahed, J.L. Sproston, R. Stanway, The performance of an electrorheological fluid in dynamic squeeze flow under constant voltage and constant field, Journal of Physics D 31 (1998) 2964–2974.
[20] A.K. El Wahed, J.L. Sproston, R. Stanway, The performance of electrorheological fluid in dynamic squeeze flow: the influence of solid phase size, Journal of Colloid and Interface Science 211 (1999) 264–280.
[21] A.K. El Wahed, J.L. Sproston, E.W. Williams, The effect of a time-dependent electric field on the dynamic performance of an electrorheological fluid in squeeze, Journal of Physics D 33 (2000) 2995–3003.
[22] S.Y. Jung, S.B. Choi, Analysis of a short squeeze-film damper operating with electrorheological fluids, Tribology Transactions 38 (4) (1995) 857–862.
[23] S. Morishita, Y.K. An, On dynamic characteristics of ER fluid squeeze film damper, JSME International Journal Series C 39 (4) (1996) 702–707.
[24] Y. Guozhi, M. Guang, F. Tong, Electro-Rheological fluid and its application in vibration control, Machine Vibration 4 (1995) 232–240.

[25] R. Stanway, J.L. Sproston, A.K. El Wahed, Applications of electrorheological fluids in vibration control: a survey, Journal of Smart Materials and Structures 5 (4) (1996) 464–482.
[26] N.D. Sims, R. Stanway, A.R. Johnson, Vibration control using smart fluids: a state-of-the-art review, Shock and Vibration Digest 31 (3) (1999) 195–205.
[27] D.J. Peel, R. Stanway, J.L. Sproston, W.A. Bullough, An ER long-stroke damper: performance modelling under quasi-static conditions, American Society of Mechanical Engineers, Design Engineering Publishing Division, DE (Vibration Control, Analysis and Identification) 84-3 (Part C) (1995) 737–744.
[28] J.P. Coulter, K.D. Weiss, J.D. Carlson, Engineering applications of electro-rheological fluids, Journal of Intelligent Material Systems and Structures 4 (1993) 248–259.
[29] E.W. Williams, S.G. Rigby, J.L. Sproston, R. Stanway, Electrorheological fluids applied to an automotive engine mount, Journal of Non-Newtonian Fluid Mechanics 47 (1993) 221–238.
[30] M.I. Friswell, J.E. Mottershead, Finite Element Model Updating in Structural Dynamics, Kluwer, Dordrecht, 1995.
[31] T.C. Jordan, M.T. Shaw, Electrorheology, IEEE Transactions Electrical Insulation 24 (5) (1989) 849–878.
[32] R.T. Bonnecaze, J.F. Brady, Yield stresses in electrorheological fluids, Journal of Rheology 36 (1992) 73–115.
[33] H. Bose, R.H.W. Hoppe, G. Mazurkevitch, Personal Communication, Computer simulations of electrorheological fluid flows, Journal of Non-Newtonian Fluid Mechanics, accepted for publication.
[34] NAG Library Reference Manual, Vol. 5, Correlation and Regression Analysis, Routine GO2 CAF NAG, Oxford.
[35] A.K. El Wahed, R. Stanway, J.L. Sproston, The influence of mechanical input amplitude on the dynamic response of an electrorheological fluid in squeeze flow, International Journal of Vehicle Design, accepted for publication.